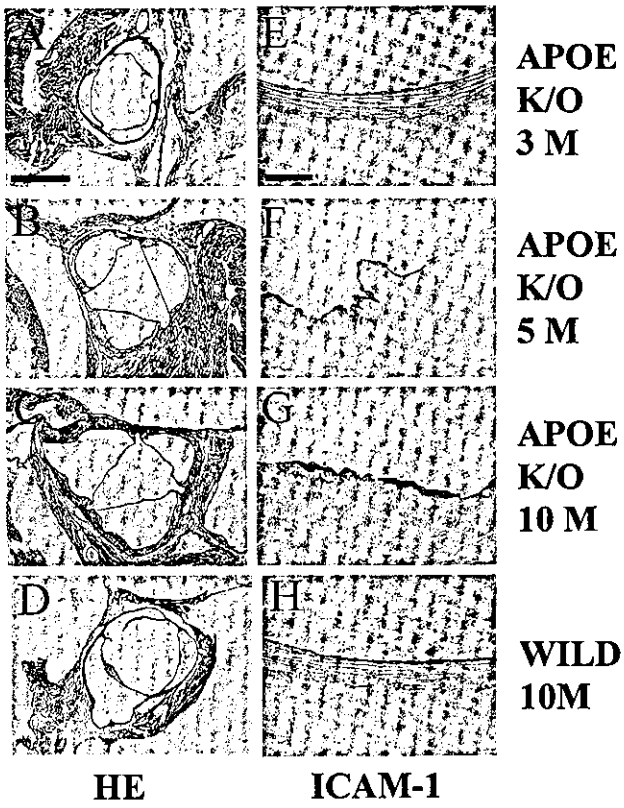

Fig. 1. Representative photographs of aortic roots from APOE-deficient mice of 3 (A), 5 (B) and 10 months (C) of age, and from wild C57BL/6 mice of 10 months of age (D). An immunoreaction for ICAM-1 on endothelial cells of aortic root is also shown (E–H). Bar in (A) 1.0 mm for (A–D). Bar in (E) 20 μm for (E–H).

$N = 8$ at 3 months; 43.5 ± 9.5 μg/ml, $N = 8$ at 5 months; 50.2 ± 14.7 μg/ml, $N = 8$ at 10 months) (Fig. 2). However, no correlation between lesion size and the level of sICAM-1 in APOE-deficient mice was found at

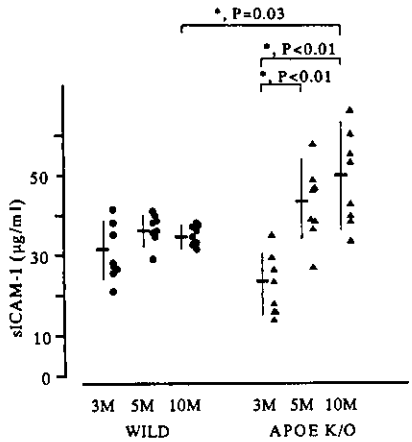

Fig. 2. sICAM-1 in wild-type and APOE-deficient mice of 3, 5 and 10 months of age. Each symbol represents the sICAM-1 value of a single mouse; the short, thick horizontal bars indicate the mean of the group and vertical bars indicate the S.D. of the group. * $P < 0.05$.

Table 1
Total plasma cholesterol (mg/dl) in APOE-deficient mice on a normal chow diet

Mouse strain	3 months	5 months	10 months
Wild	110.8 ± 46.1(6)	94.4 ± 11.0(6)	124.0 ± 19.1(6)
APOE$^{-/-}$/ICAM-1$^{+/+}$	486.8 ± 103.6 (8)	524.5 ± 213.4 (8)	455.7 ± 85.3 (8)
APOE$^{-/-}$/ICAM-1$^{-/-}$	443.0 ± 101.3 (8)	483.4 ± 166.3 (8)	503.6 ± 79.7 (8)

The values represent mean ± S.D. The values in parentheses represent the number of mice evaluated.

5 or 10 months because of variation in the level of sICAM-1 in each APOE-deficient mouse. Endothelial expression of ICAM-1 was strongly positive over the atheromatous plaque at 5 and 10 months of age in APOE-deficient mice, while ICAM-1 expression was detected in virtually all endothelial cells overlying the vessel without lesions after 3 months in APOE-deficient mice, and at any age in wild-type mice (Fig. 1).

3.2. Atherosclerotic lesion formation in ICAM-1-deficient mice

To study the role of ICAM-1 in atherosclerotic lesion development, we first made sure that the APOE$^{-/-}$/ICAM-1$^{+/+}$ and APOE$^{-/-}$/ICAM-1$^{-/-}$ mice showed comparable levels of cholesterol in the blood. The total plasma cholesterol was around 500 mg/dl in APOE$^{-/-}$ mice, independent of ICAM-1 genotype (Table 1), while it was about 100 mg/dl in wild-type mice. The ICAM-1 genotype was again confirmed in the immunohistochemical reaction for ICAM-1 in the atherosclerotic sections, as ICAM-1 was expressed strongly on the endothelium over the lesions in APOE$^{-/-}$/ICAM-1$^{+/+}$ mice, but not on the endothelium in the atheromatous plaque of APOE$^{-/-}$/ICAM-1$^{-/-}$ mice (Fig. 3). Atherosclerotic lesions were generally smaller in APOE$^{-/-}$/ICAM-1$^{-/-}$ mice than in APOE$^{-/-}$/ICAM-1$^{+/+}$ mice at any age, and the significance was found at 5 and 10 months of age (Fig. 4: $P = 0.21$ at 3 months, $P = 0.02$ at 5 months and $P = 0.01$ at 10 months with Mann–Whitney U test). At 3 months of age, small lesions in the cusp region were usually less in APOE$^{-/-}$/ICAM-1$^{-/-}$ mice (Fig. 3, an arrow), and at 5 months, the athersoclerotic lesions in both the cusp region and ascending aorta (Fig. 5, an arrow) were less severe in APOE$^{-/-}$/ICAM-1$^{-/-}$ mice. After 10 months, both APOE$^{-/-}$/ICAM-1$^{+/+}$ and APOE$^{-/-}$/ICAM-1$^{-/-}$ mice showed complex fibrous lesions with necrotic cores and calcification (Fig. 5, arrowheads). Although the similar size of atherosclerotic lesions was observed in the cusp region

(Fig. 3C and 3G), quantitation of lesion size from the aortic root to the ascending aorta showed a statistically significant difference between ICAM-1-positive and -negative mice (Fig. 5).

4. Discussion

It remained unclarified whether sICAM-1 showed any correlation with the degree of atherosclerosis in an animal model as it did in a clinical study [7]. Only recently, Cayatte et al. [15] demonstrated that treatment with a thromboxane receptor antagonist for 11 weeks inhibits atherogenesis, as well as serum ICAM-1 levels. In the present study, we demonstrated for the first time that sICAM-1 levels remained constant during almost whole life span (from 3 to 10 months) in the control mice, but the value elevated in APOE-deficient mice of 5 months or older when atherosclerotic lesions were marked in the aortic root and ascending aorta. Although our results suggested a relationship between sICAM-1 levels and atherosclerotic progression, ICAM-1 was expressed not only over lesions, but also in virtually all endothelial cells without any lesions.

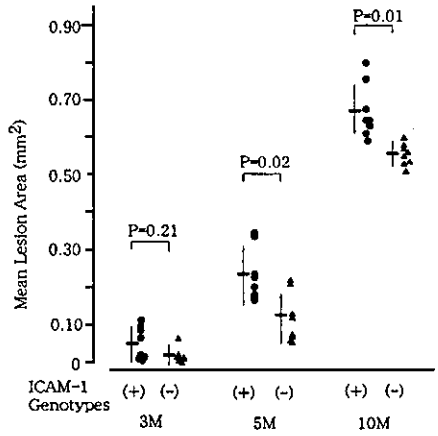

Fig. 4. Atherosclerotic lesion area in APOE$^{-/-}$/ICAM-1$^{+/+}$ and APOE$^{-/-}$/ICAM-1$^{-/-}$ mice. Microscopic cross sections (10 μm in thickness) of the proximal aortic root were stained with hematoxylin and eosin and quantitated by morphometry. Each symbol represents the average lesion area from eight sections of a single mouse; the short, thick, horizontal bars indicate the mean of the group and the vertical bars indicate the SD of the group.

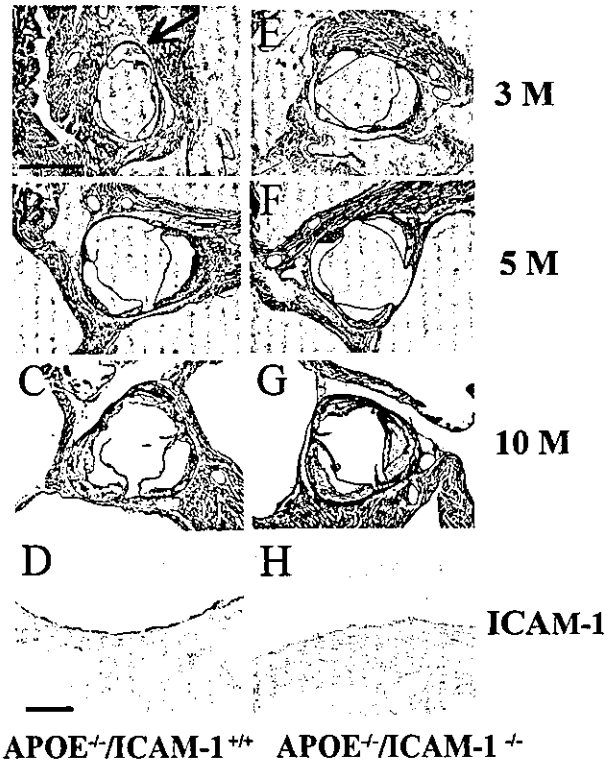

Fig. 3. Representative photographs of aortic roots from APOE$^{-/-}$/ICAM-1$^{+/+}$ and APOE$^{-/-}$/ICAM-1$^{-/-}$ mice of 3 (A and E), 5 (B and F) and 10 months (C and G) of age. An immunoreaction for ICAM-1 on endothelial cells of aortic root in APOE$^{-/-}$/ICAM-1$^{+/+}$ (D) and APOE$^{-/-}$/ICAM-1$^{-/-}$ (H) mice at 5 months of age is also shown. The arrow indicates a small lesion in an APOE$^{-/-}$/ICAM-1$^{+/+}$ mouse. Bar in (A) 1.0 mm for (A–C) and (E–F). Bar in (D) 20 μm for (D) and (H).

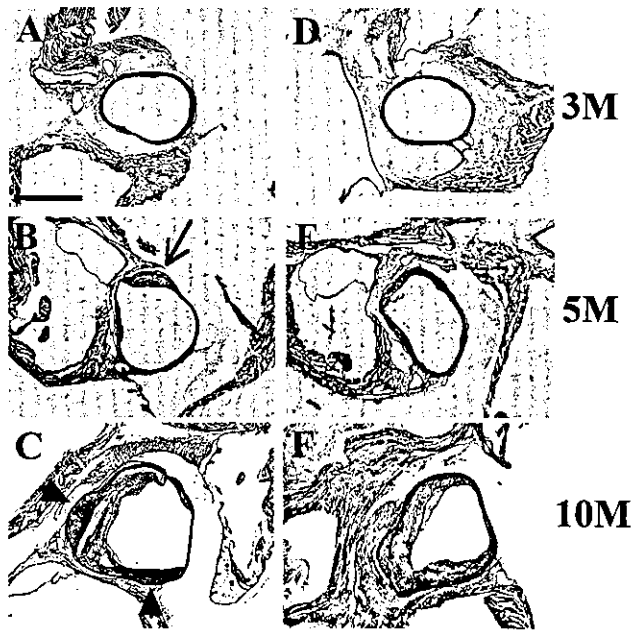

Fig. 5. Representative photographs of the ascending aorta from APOE$^{-/-}$/ICAM-1$^{+/+}$ (A–C) and APOE$^{-/-}$/ICAM-1$^{-/-}$ (D–F) mice of 3 (A and D), 5 (B and E) and 10 (C and F) months of age. The arrow and arrowheads indicate an atherosclerotic lesion and calcification, respectively, in an APOE$^{-/-}$/ICAM-1$^{+/+}$ mouse. Bar = 1.0 mm.

Therefore, elevated sICAM-1 levels in APOE-deficient mice may be explained by a systemic inflammatory response which could be a key factor in atherosclerotic progression [16], and not by increased ICAM-1 expression on endothelial cells. However, immunohistochemistry may not be the best technique to study ICAM-1 expression, and future studies examining transcription level of ICAM-1 gene will be required to clarify ICAM-1 expression in atherosclerotic lesions.

Whether sICAM1 levels reflect endothelial expression of ICAM-1 and macrophage accumulation in the plaque or not, there is accumulating evidence from both clinical and experimental examinations that ICAM-1 is closely involved in the progression of atherosclerosis [3,7,9–11]. Treatment with neutralizing antibodies against ICAM-1 in APOE$^{-/-}$ mice [17], or hypercholesterolemic rats [18], as well as ICAM-1 deficiency in C57BL/6 mice fed a high fat diet [11] and APOE$^{-/-}$ mice [9], all showed substantial protection against atherosclerosis. However, the examined point was usually up to 20 weeks in APOE$^{-/-}$ mice, and therefore, it remains unclear whether therapeutic inhibition of ICAM-1 reduces or delays the progression of atherosclerosis in the more advanced stage. In the present study, we compared atherosclerotic lesion size between ICAM-1-positive and -negative APOE-deficient mice from 3 to 10 months of age. Because the whole area of fibrous complex lesions in advanced atherosclerosis is not stained with oil red, we used a quantitative histological method to evaluate the lesion size. We demonstrated that ICAM-1 deficiency was protective at 5 and 10 months of age. The result is in apparent agreement with recent papers that demonstrated the reduction of lesions in the aortic tree due to ICAM-1 deficiency in APOE-deficient mice [9,10]. However, ICAM-1 may be less involved in advanced atherosclerosis than P-selectin, because Dong et al. [19] recently demonstrated that the absence of P-selectin in APOE-deficient mice showed prominent protection against advanced atherosclerosis.

There are several points to be taken into account in the interpretation of our results. Firstly, it should be noted that the ICAM-1-deficient mice used in this study were later found to express residual amounts of ICAM-1 by alternative splicing of RNA [20]. Although the amount of ICAM-1 protein in the lungs of the mutant mice was less than 1% of that found in the wild type mice, and expression of ICAM-1 on endothelial cells was almost null in the mutant mice (Fig. 2), it is possible that some inducible ICAM-1 participated in the progression of atherosclerosis in the APOE$^{-/-}$/ICAM-1$^{-/-}$ mice. Secondly, our results are limited to the aortic root and ascending aorta. Although it was reported that the extent of lesions in the entire aorta measured by surface area showed a close correlation with that at the aortic origin measured as the average lesion area per cross-section [21], the effect of ICAM-1 deficiency in lesions of coronary and cerebral arteries, which are much more important in cardiovascular events than the aorta, must be examined. Thirdly, although only a weak difference of lesion size was seen in ICAM-1-positive and -negative mice in this study, the stability of atheromatous plaque, which is believed to be important as a trigger for vessel occlusion and ischemic events, may be different.

In conclusion, we demonstrated higher levels of sICAM-1 in APOE$^{-/-}$ mice of 5 months or older, and a mild protective effect of ICAM-1 deficiency against atherosclerosis during the whole life span. Our results support the importance of ICAM-1 in the formation and progression of atherosclerosis, but also suggested the limitations of anti-ICAM-1 therapy in preventing advanced atherosclerosis.

Acknowledgements

The authors thank Mr Nobuo Katsube of Ono Pharamaceutical Company for helpful discussion, and Y. Imaeda and R. Morimoto for their secretarial assistance. The present study was supported in part by Takeda Science Foundation and Smoking Research Foundation of Japan.

References

[1] Ross R. Atherosclerosis—an inflammatory disease. N Engl J Med 1999;340:115–26.
[2] Dong ZM, Wagner DD. Leukocyte-endothelium adhesion molecules in atherosclerosis. J Lab Clin Med 1998;132:369–75.
[3] Posten RN, Haskard DO, Coucher JR, Gall NP, Johnson-Tidey RR. Expression of intercellular adhesion molecule-1 in atherosclerotic plaques. Am J Pathol 1992;140:665–73.
[4] DeGrabe TJ. Expression of inflammatory mediators and adhesion molecules in human atherosclerotic plaque. Neurology 1997;49(Suppl 4):S15–9.
[5] Iiyama K, Hajra L, Iiyama M, Li H, DiChiara M, Medoff BD, Cybulsky MI. Patterns of vascular cell adhesion molecule-1 and intercellular adhesion molecule-1 expression in rabbit and mouse atherosclerotic lesions and at sites predisposed to lesion formation. Circ Res 1999;85:199–207.
[6] Nakashima Y, Raines EW, Plump AS, Breslow JL, Ross R. Upregulation of VCAM-1 and ICAM-1 at atherosclerosis-prone sites on the endothelium in the ApoE-deficient mouse. Arterioscler Thromb Vasc Biol 1998;18:842–51.
[7] Rohde LK, Lee RT, Rivero J, Jamacochian M, Arroyo LH, Briggs W, Rifai N, Libby P, Creager MA, Ridker PM. Circulating cell adhesion molecules are correlated with ultrasound-based assessment of carotid atherosclerosis. Arterioscler Thromb Vasc Biol 1998;18:1765–70.
[8] Ridker PM, Hennekens CH, Ritman-Johnson B, Stamper MJ, Allen J. Plasma concentration of soluble intercellular adhesion molecule 1 and risks of future myocardial infarction in apparently healthy men. Lancet 1998;351:88–92.
[9] Collins RG, Velji R, Guevara NV, Hicks MJ, Chan L, Beaudet AL. P-selectin or intercellular adhesion molecule (ICAM)-1 defi-

ciency substantially protects against atherosclerosis in apolipoprotein E-deficient mice. J Exp Med 2000;191:189–94.
[10] Bourdillon MC, Poston RN, Covacho C, Chignier E, Bricca G, McGregor JL. ICAM-1 deficiency reduces atherosclerosis lesions in double-knockout mice (ApoE$^{-/-}$/ICAM-1$^{-/-}$) fed a fat or a chow diet. Arterioscler Thromb Vasc Biol 2000;20:2630–5.
[11] Nageh M, Sandberg KR, Marotti KR, Lin AH, Melchior EP, Bullard DC, Beaudet AL. Deficiency of inflammatory cell adhesion molecules protects against atherosclerosis in mice. Arterioscler Thromb Vasc Biol 1997;17:1517–20.
[12] Zhang SH, Reddick RL, Piedrahita JA, Maeda N. Spontaneous hyperchelosterolemia and arterial lesions in mice lacking apolipoprotein E. Science 1992;258:468–71.
[13] Sligh JE, Ballantyne CM, Rich SS, Hawkins HK, Smith CW, Bradley A, Beaudet AL. Inflammatory and immune responses are impaired in ICAM-1 deficient mice. Proc Natl Acad Sci USA 1993;90:8529–33.
[14] Paigen B, Morrow A, Holmes PA, Mitchell D, Wiiliams RA. Quantitative assessment of atherosclerotic lesions in mice. Atherosclerosis 1987;68:231–40.
[15] Cayatte AJ, Du Y, Oliver-Krasinski J, Lavielle G, Verbeuren TJ, Cohen RA. The thromboxane receptor antagonist S18886 but not asppirin inhibits atherogenesis in Apo E-deficient mice. Arterioscle Thromb Vasc Biol 2000;20:1724–8.
[16] Danesh J, Collins R, Peto R. Chronic infections and coronary heart disease: is there a link? Lancet 1997;350:430–6.
[17] Patel SS, Thiagarajan R, Willerson JT, Yeh ETH. Inhibition of α4 integrin and ICAM-1 markedly attenuate macrophage homing to atherosclerosis plaques in ApoE-deficient mice. Circulation 1998;97:75–81.
[18] Nie Q, Fan J, Haraoka S, Shimokama T, Watanabe T. Inhibition of mononuclear cell recruitment in aortic intima by treatment with anti-ICAM-1 and anti-LFA-1 monoclonal antibodies in hypercholesterolemic rats: Implications of the ICAM-1 and LFA-1 pathway in atherogenesis. Lab Invest 1997;77:469–82.
[19] Dong ZM, Brown AA, Wagner DD. Prominent role of P-selectin in the development of advanced atherosclerosis in ApoE-deficient mice. Circulation 2000;101:2290–5.
[20] King PD, Sandberg ET, Selvakumar A, Fang P, Beaudet AL, Dupont B. Novel isoforms of murine intercellular adhesion molecule-1 generated by alternative RNA splicing. J Immunol 1995;154:6080–93.
[21] Tangirala RK, Rubin EM, Palinski W. Quantitation of atherosclerosis in murine models: correlation between lesions in the aortic origin and in the entire aorta, and differences in the extent of lesions between sexes in LDL receptor-deficient and apolipoprotein E-deficient mice. J Lipid Res 1995;36:2320–8.

Detection of Misery Perfusion With Split-Dose ^{123}I-Iodoamphetamine Single-Photon Emission Computed Tomography in Patients With Carotid Occlusive Diseases

Masao Imaizumi, MD; Kazuo Kitagawa, MD, PhD; Kazuo Hashikawa, MD, PhD; Naohiko Oku, MD, PhD; Tadamasa Teratani, MD; Masashi Takasawa, MD; Takuya Yoshikawa, MD; Piao Rishu, MD; Toshiho Ohtsuki, MD, PhD; Masatsugu Hori, MD, PhD; Masayasu Matsumoto, MD, PhD; Tsunehiko Nishimura, MD, PhD

Background and Purpose—Patients with carotid occlusive disease and stage 2 cerebral hemodynamic failure, characterized by an increased oxygen extraction fraction (OEF) as measured by positron emission tomography (PET) and otherwise known as misery perfusion, have a high risk of cerebral ischemia and subsequent stroke. In clinical practice, the detection of patients with misery perfusion through the use of widely available, noninvasive, and cost-effective modalities such as single-photon emission computed tomography (SPECT) is extremely important.

Methods—We evaluated the relationships between the regional hemodynamic status of cerebral circulation, measured with split-dose [^{123}I] *N*-isopropyl-p-iodoamphetamine SPECT (^{123}I-IMP SPECT) and an acetazolamide challenge, and hemodynamic parameters, including OEF measured with PET, in 27 patients with both unilateral and bilateral carotid occlusive diseases.

Results—A significant negative correlation was found between the SPECT-measured cerebrovascular reserve after acetazolamide administration and both the PET-measured OEF and cerebral blood volume. Neither the cerebrovascular reserve nor the cerebral blood flow index, when expressed as a SPECT-measured cerebrum-to-cerebellum ratio, was useful for detecting lesions with an elevated OEF. However, a combination of the cerebrovascular reserve and cerebral blood flow index showed high sensitivity, specificity, and positive predictive value for the detection of misery perfusion.

Conclusions—Our study suggests that split-dose ^{123}I-IMP SPECT with an acetazolamide challenge could be useful for screening patients with misery perfusion in carotid occlusive diseases. (***Stroke.* 2002;33:2217-2223.)**

Key Words: acetazolamide ■ hemodynamics ■ tomography, emission computed

Severe atherosclerotic disease of the carotid and vertebral arteries or their intracranial branches may cause hemodynamic impairment of the distal cerebral circulation. Several studies have shown that patients with hemodynamics have a high risk of subsequent ischemic stroke[1–3]; therefore, the identification and treatment of high-risk patients could help to prevent stroke. Among the various methods of hemodynamic assessment, positron emission tomography (PET) is the most reliable tool for the quantitative assessment of blood supply and metabolic demand. When PET with ^{15}O gases is used, the hemodynamic effect can be categorized into 3 stages: stage 0, normal cerebral hemodynamics; stage 1, autoregulatory vasodilatation in which the cerebral blood volume (CBV) is increased and other parameters are normal; and stage 2, in which the cerebral blood flow (CBF) is reduced and the oxygen extraction fraction (OEF) is increased to maintain the cerebral metabolic rate of oxygen ($CMRO_2$) and CBV.[4] Stage 2 has been called "misery perfusion" and represents an inadequate blood supply relative to metabolic demand.[5] The presence of an increased OEF lesion can be a predictor of subsequent ischemic stroke.[2,3] In clinical practice, the detection of misery perfusion in patients with carotid occlusive disease is important for the prevention of stroke and may be performed with widely available, noninvasive, and cost-effective modalities such as single-photon emission computed tomography (SPECT). However, the conventional method of measuring cerebrovascular reserve (CVR) with SPECT takes >2 days to perform and requires arterial blood sampling. We have developed a split-dose [^{123}I] *N*-isopropyl-p-iodoamphetamine (^{123}I-IMP) SPECT method, followed by an acetazolamide (ACZ) challenge, that enables noninvasive and semiquantitative measurements of regional CBF and CVR to be performed in 1 hour.[6,7] Although several studies have shown a relationship between impaired CVR measured

Received March 18, 2002; final revision received May 3, 2002; accepted May 7, 2002.

From the Division of Tracer Kinetics (M.I., N.O., T.T., P.R., T.N.) the Department of Internal Medicine and Therapeutics (K.K., K.H., M.T., T.Y., T.O., M.H., M.M.), Osaka University Graduate School of Medicine, Suita, Osaka, Japan.

Correspondence to Masao Imaizumi, MD, Division of Tracer Kinetics, Osaka University Graduate School of Medicine, 2-2, Yamadaoka, Suita City, Osaka, 565-0871, Japan. E-mail imaizumi@tracer.med.osaka-u.ac.jp

Stroke is available at http://www.strokeaha.org

DOI: 10.1161/01.STR.0000027638.19392.7E

Patient Characteristics

Patient	Age, y	Sex	Neurological Deficits	Disease	Angiographical Findings	MRI Findings
1	72	M	None	Asymptomatic	R ICAS	R BG
2	69	F	L sensory disturbance	CI	R MCAO	R BG~CR
3	70	F	Dysarthria	CI	L ICAO	L BG~CR
4	65	M	None	Asymptomatic	R ICAS	None
5	73	F	Visual field defect	CI	L ICAS	R temporal~occipital subcortex
6	59	M	L sensory disturbance	TIA	R MCAS, & L ICAS	Bil BG~deep white matter
7	67	M	Syncope	CI	R ICAO	Bil BG
8	62	M	R sensory disturbance	CI	L MCAS	L BG
9	61	M	Dizziness	CI	Bil ICAS	Bil deep white matter
10	75	F	Dizziness	CI	L MCAS	L CR
11	61	F	R hemiparesis	TIA	L ICAO	None
12	63	F	None	Asymptomatic	L ICAS	None
13	28	F	L hemiparesis	TIA	Bil MCAS	None
14	31	F	R hemiparesis	CI	Bil ICAS	R BG
15	60	M	Perseveration	CI	L MCAS	L BG
16	67	M	Dizziness	Asymptomatic	L ICAO	L BG, L frontoparietal subcortex
17	54	M	Visual field defect	CI	R MCAS	R BG
18	63	F	None	Asymptomatic	L ICAS	Bil BG~CR
19	68	M	R hemiparesis	TIA	L MCAS	Pons
20	66	M	R hemiparesis	CI	L MCAO, R ICAS	Bil BG
21	64	F	L hemiparesis	CI	R ICAO	R frontal lobe
22	70	M	R hemiparesis	CI	R ICAO	L BG
23	35	M	L hemiparesis	TIA	R ICAO	None
24	63	F	R hemiparesis & motor aphasia	CI	L ICAS	L BG~CR
25	69	F	L hemiparesis	TIA	R ICAO	None
26	54	F	Motor aphasia	CI	L MCAO	L CR
27	71	M	L hemiparesis	TIA	R ICAO	R temporal, parietooccipital subcortex

Asymptomatic indicates asymptomatic carotid artery disease; ICAS, internal carotid artery stenosis; BG, basal ganglia; CI, cerebral infarction; MCAO, MCA occlusion; CR, corona radiata; ICAO, internal carotid artery occlusion; TIA, transient ischemic attack; MCAS, MCA stenosis; and Bil, bilateral.

by ACZ injection or CO_2 inhalation with SPECT and an increased OEF measured by PET,[8-11] it remains unsettled as to whether an ACZ challenge and split-dose ^{123}I-IMP SPECT can be used to detect patients with misery perfusion. Therefore, the purpose of this study was to clarify the relationship between the CVR and CBF index measured by routine split-dose ^{123}I-IMP SPECT and the hemodynamic parameters measured by PET in 27 carotid occlusive diseases.

Subjects and Methods

Enrollment in this study began on February 16, 2000, and ended on July 10, 2001. A total of 43 consecutive patients with chronic cerebrovascular diseases were examined with both SPECT and PET during this period at the Osaka University Medical School Hospital. Before the SPECT and PET examinations, each subject underwent neurological and neuroradiological evaluations, including an evaluation for occlusive cerebrovascular disease by duplex carotid ultrasonography, MRI, MR angiography (MRA), and cerebral angiography. The MRI examination was performed in 5-mm-thick sections along the orbitomeatal plane with a 1.5-T unit. Infarction was defined as a focal area with prolonged T1 and T2 relaxation times. The interval between the MRI study and the SPECT and PET studies was <30 days. The SPECT study was performed at least 4 weeks after the patient's most recent clinical episode, once the neurological condition had stabilized. Two neuroradiologists who were unaware of the patients' medical histories and diagnoses independently reviewed the MRI, SPECT, and PET images. A cerebral angiography was performed in all patients. The maximum percentage of stenosis and the presence of ulceration were evaluated according to the recommendations of the North American Symptomatic Carotid Endarterectomy Trial.[12]

The mechanism of stroke was clinically diagnosed in each patient and classified according to the National Institute of Neurological Disorders and Stroke classification of cerebrovascular disease III.[13] Patients with cardioembolic infarctions were excluded from the study. Finally, we selected 27 consecutive patients (13 men, 14 women; mean±SD age, 61.5±12.1 years) with occlusion or stenosis of the internal carotid artery or the main trunk of the middle cerebral artery (MCA) to be included in this study. Fifteen patients had a small cerebral infarction (<15 mm in diameter), 7 had transient ischemic attacks, and 5 had asymptomatic carotid artery disease. The clinical feature, angiographic findings, and MRI findings are summarized in the Table.

SPECT Imaging

We used a high-performance, 4-head rotating gamma camera equipped with a low-energy, general-purpose, parallel-hole collimator with a spatial resolution of 13.0-mm full width at half-maximum (Gamma View SPECT 2000H, Hitachi Medical Co). Data were acquired in a continuous rotating mode in reciprocal directions at 20 seconds per revolution for 66 minutes from 96 directions in a 64×64 matrix. The transaxial images were reconstructed with a Butterworth

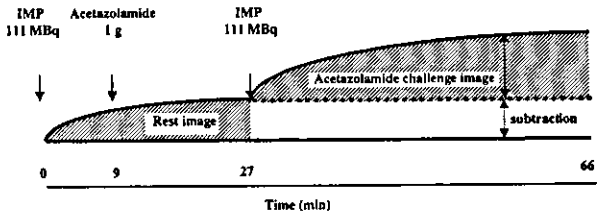

Figure 1. Split-dose IMP-SPECT (dynamic imaging protocol). During an ≈1-hour SPECT acquisition, double injections of 111 MBq ^{123}I-IMP were performed before and after ACZ administration. Two perfusion images (resting and ACZ challenge) were obtained with the subtraction technique.

filter. During the dynamic SPECT, 111 MBq ^{123}I-IMP (Nihon Mediphysics) was intravenously injected at the start of imaging, and 1 g ACZ (Diamox, Lederle Ltd) was slowly injected intravenously over a 1-minute period 9 minutes after the initial ^{123}I-IMP injection. An additional 111 MBq ^{123}I-IMP was injected 27 minutes after the start of imaging. Two perfusion images, resting and vasodilated, were obtained with the subtraction technique (Figure 1).

PET Imaging

All patients were scanned with a Headtome V/SET 2400W system (Shimadzu Co, Ltd), which acquires 63 slices with an interslice distance of 3.1 mm. All scans were performed at a resolution of 3.7-mm full width at half-maximum in the transaxial direction and at 5 mm in the axial direction. The patient's head was fixed in place with a head holder and was positioned with light beams to obtain transaxial slices parallel to the orbitomeatal line. Before the PET study, germanium-68–gallium-68 transmission scanning was performed for 10 minutes for attenuation correction. Images were reconstructed with an ordered-subset expectation maximization algorithm (12 iterations with 4 ordered subsets). For the ^{15}O-labeled gas steady-state method, $C^{15}O_2$ (550 MBq/min) and $^{15}O_2$ (1300 MBq/min) were inhaled through a mask. The scan time was 9 minutes, and arterial blood was manually sampled from the radial artery 4 times during each scan. The concentration of the radiotracer activity in the whole blood and plasma was measured with a well counter; the arterial blood hematocrit, hemoglobin concentration, Pa_{O_2}, and Pa_{CO_2} were also measured. Inhalation of 2000 MBq $C^{15}O$ and a 9-minute scanning period were used to measure the CBV. Arterial sampling was manually performed 3 times during the scanning, and the radiotracer activity in whole blood was measured. CBF, CMR_{O_2}, and OEF were calculated from the steady-state method, and CMR_{O_2} and OEF were corrected according to the CBV. The study protocol was in accordance with the standard ethics guidelines of Osaka University Medical School, and written, informed consent was obtained from all subjects.

Data Analysis

All SPECT and PET data were analyzed with the Dr. View pro5.0 image analysis software system (Asahi Kasei Joho System Co, Ltd) running on a UNIX system and an Indigo 2 station (Silicon Graphics). The region-of-interest (ROI) analysis in this study is illustrated in Figure 2. Circular ROIs, 20 mm in diameter, were placed over the cortex at the levels of the basal ganglia (lower MCA territory), parietal lobe (upper MCA territory), and cerebellar hemispheres in the SPECT and PET images of each patient. To match the slice thickness, the ROIs in each level of the MCA territories were placed over 3 slices (12 mm) on the SPECT images and over 4 slices (12.5 mm) on the PET images. Finally, 108 regions were investigated in 27 patients (4 regions in each patient: right and left, and upper and lower MCA). In the SPECT study, all ROIs generated in the resting image were transferred to the ACZ-challenge image. In the PET study, all of the ROIs generated in the CBF images were transferred to the OEF, CMR_{O_2}, and CBV images. The following equation was used to estimate the percentage increase in regional CBF induced by the ACZ challenge in the form of the CVR: CVR equals ACZ challenge SPECT count minus resting SPECT count divided by resting SPECT count. To estimate the resting CBF, the cerebral cortical ROI counts were normalized to those of the cerebellar hemisphere by use of the higher counts, which eliminated any effects of crossed cerebellar diaschisis.

Seven age-matched patients who complained of nonfocal neurological symptom (dizziness or headache) and who showed no ischemic lesions after MRI and no stenotic lesions in their major cerebral arteries after MRA underwent SPECT examination to determine their control values. The normal control values for CVR and cerebrum-to-cerebellum ratio (CBF index) for the MCA territories made a normal distribution; they were 0.69 ± 0.23 and 0.83 ± 0.09, respectively. The mean CVR after ACZ challenge in the normal subjects was 0.69 in our study, which agrees with previous reports.[14,15] The CBF index and CVR values were judged to be abnormal when they were beyond the range of the mean±2 SD range of the normal control subjects. The 108 MCA territories examined were divided into 2 groups according to the angiographic findings. Group A consisted of MCA areas with a severe stenotic lesion (>70%) in the ipsilateral internal carotid artery system, whereas group NA consisted of those with less or no stenotic lesion. All regions were also classified into 2 groups according to their SPECT CVR values: a reduced CVR group with a CVR of <0.23 (mean−2 SD) and a normal CVR group with a CVR of ≥0.23. Because normal values obtained from healthy control subjects were not available, we used PET parameter values obtained from 7 patients with no infarction and no severe stenosis or occlusion (<50%) who were suffering from nonspecific brain symptoms without focal signs (ie, preoperation for cerebral aneurysm, headache, dizziness, and syncope) as the normal values: CBF, 46.9 ± 11.3 mL · 100 g^{-1} · min^{-1} (mean±SD); OEF, 44.1 ± 4.62%; CMR_{O_2}, 3.39 ± 0.82 mL · 100 g^{-1} · min^{-1}; and CBV, 4.22 ± 0.75%. All regions were classified into 3 groups on the basis of their OEF values: normal group, OEF <48.7% (mean+1 SD of the mean OEF value); slightly increased OEF group, 48.7%≤OEF<53.3% (mean+2 SD of the mean OEF value); and an increased OEF group, OEF ≥53.3%. The increased OEF value was compatible with that beyond the upper 95% confidence limits defined in healthy volunteers.[3] We assessed the relationship between the SPECT and PET parameters in the MCA territories using linear

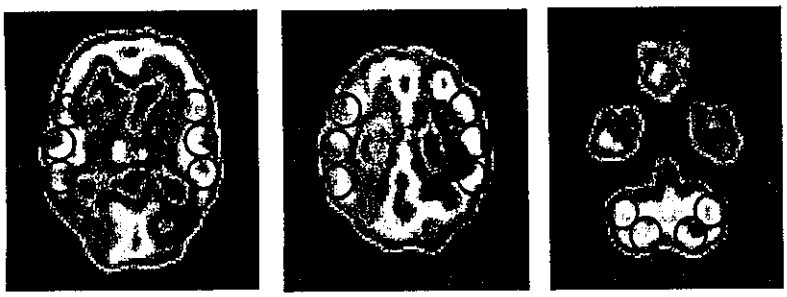

Figure 2. ROI settings. Circular ROIs, 20 mm in diameter, were placed over the cortex at the levels of the basal ganglia (lower MCA territory), parietal lobe (upper MCA territory), and cerebellum in the SPECT and PET images of each patient.

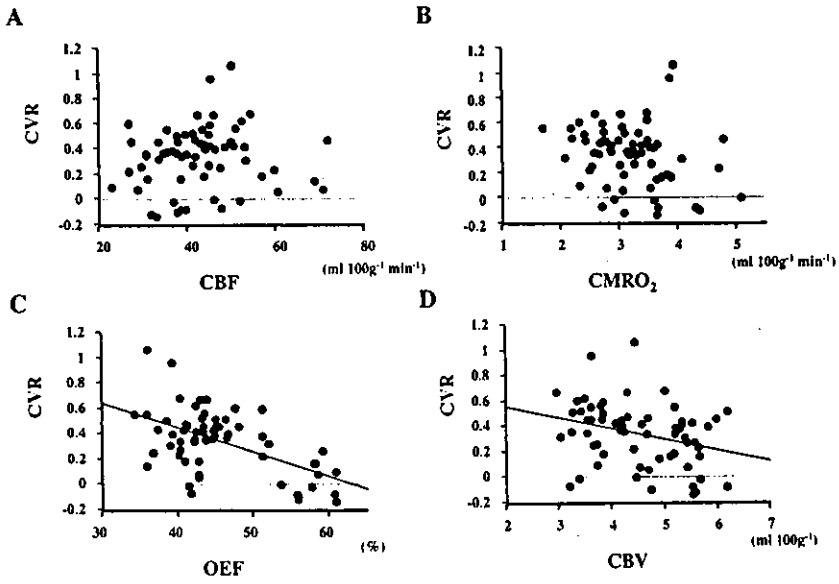

Figure 3. Relationship between CVR and PET parameters on the affected side (group A). A, CBF; B, $CMRo_2$; C, OEF; D, CBV. We compared CVR and PET parameters in group A (n=64). A significant negative correlation was observed between CVR and OEF (C, $r=-0.549$, $P<0.0001$) and between CVR and CBV (D, $r=-0.313$, $P<0.0117$). CBF (A) and $CMRo_2$ (B) were not correlated with the CVR.

regression analysis and Pearson's correlation coefficient. All data are expressed as mean±SD. Differences in data between groups were statistically evaluated with an unpaired *t* test. Differences with values of $P<0.05$ were considered to be statistically significant.

Results

Comparison of SPECT and PET Parameters

Of the 108 ROIs in all MCA territories, 64 ROIs were on an affected side (group A), and 44 ROIs were on a nonaffected side (group NA), because 5 patients with bilateral carotid disease were included. We compared the CVR and PET parameters in group A and found a significant negative correlation between CVR and OEF ($r=-0.549$, $P<0.0001$; Figure 3) and between CVR and CBV ($r=-0.313$, $P<0.0117$; Figure 3). CBF and $CMRo_2$ were not correlated with the CVR (Figure 3).

Detection of Stage 2 Cerebral Hemodynamic Failure With Semiquantitative SPECT Analysis in Group A

Figure 4 shows the typical MRI, MRA, SPECT, and PET images of a stage 2 patient. The areas of increased OEF and CBV (misery perfusion) on the PET images correspond with those of decreased CVR on the SPECT images. The lesions were classified into 3 groups according to their PET-evaluated OEF values, and each value was plotted according to the CBF index at rest and the CVR values obtained in the SPECT study (Figure 5). When the CVR cutoff value was set at 0.23 (mean−2 SD; broken line), the sensitivity of the measurement was 91% (10 of 11), and the specificity was 83% (44 of 53); however, the positive predictive value was only 53% (10 of 19) for detection of lesions with an increased OEF. When the CBF index cutoff value was set at 0.65 (mean−2 SD; dotted line), the sensitivity of the measurement was low (5 of 11, 45%). Therefore, neither the CBF index nor CVR value alone was effective in detecting lesions with an increased OEF. However, when a CVR cutoff value of 0.23 (mean−2 SD) and a CBF index cutoff value of 0.83 (normal value) (thick line) were used, the sensitivity of this combined measurement was 82% (9 of 11), the specificity was 96% (51 of 53), and the positive predictive value was 82% (9 of 11).

Discussion

Because stage 2 cerebral hemodynamic failure, characterized by an elevated OEF and also known as misery perfusion, significantly increases the risks of stroke and ipsilateral ischemic stroke,[2,3] patients with misery perfusion must be detected in clinical practice through the use of widely available modalities such as SPECT. However, a single measurement of CBF alone with SPECT is insufficient to assess the cerebral hemodynamic status in patients with carotid occlusive diseases. Therefore, CVR is usually assessed by paired blood flow measurements, with the initial measurement performed at rest and the second measurement performed after a vasodilatory stimulus such as hypercapnia, an ACZ challenge, or physiological tasks. Although a dissociation between the CBF response to hypercapnia, ACZ, or neural activation has been reported in patients with carotid occlusive disease,[16,17] ACZ increases the arterial-to-capillary blood volume and CBF without changing the $CMRo_2$ and other physiological parameters.[18] Only a few studies have investigated the relationship between ACZ reactivity and OEF.[10,11] Some investigators have reported no significant relationship between O^{15} H_2O PET-measured changes in CBF after an ACZ challenge and quantitative OEF values.[19] Conversely, the most consistent results have been published by Hirano et al,[10] who reported that a reduced regional CVR on IMP SPECT was strongly correlated with an elevated OEF and suggested that a significantly reduced regional CVR represents stage 2 hemodynamic failure with an increased OEF on PET. Hirano et al used conventional ^{123}I-IMP SPECT with arterial sampling and an asymmetry index comparing affected and nonaffected sides after the ACZ test. However, cerebral hemodynamics may be disturbed in the nonaffected hemisphere as a result of collateral circulation, suggesting that the CVR in the contralateral hemisphere cannot be used as an internal control for each patient, even in unilateral

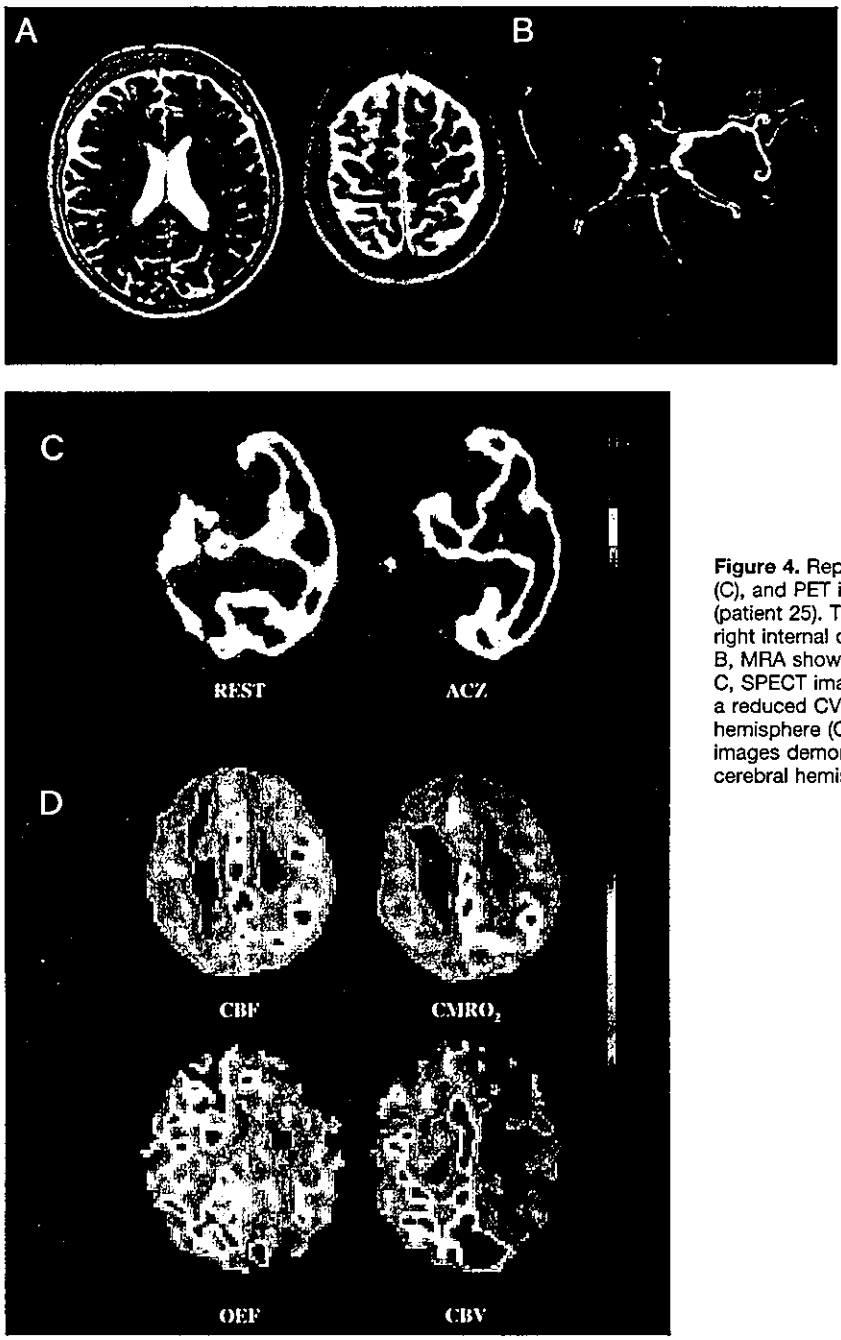

Figure 4. Representative MRI (A), MRA (B), SPECT images (C), and PET images (D) in a patient with misery perfusion (patient 25). This patient is a 69-year-old woman with a right internal carotid occlusion. A, MRI shows no infarction. B, MRA shows occlusion of right internal carotid occlusion. C, SPECT images demonstrate a reduced CBF at rest and a reduced CVR after ACZ challenge in the right cerebral hemisphere (CBF index=0.62, CVR=−0.07). D, PET images demonstrate an elevated OEF and CBV in the right cerebral hemisphere (OEF=61%, CBV=5.8%).

carotid occlusive disease.[20] Furthermore, patients with bilateral carotid disease cannot be evaluated with an asymmetry index for ^{123}I-IMP SPECT after an ACZ challenge.

We have developed a split-dose ^{123}I-IMP SPECT method for evaluating CVR after cerebral vasodilatory stimuli and have modified the procedure so that invasive arterial blood sampling is not required.[6,7,21,22] In contrast to the conventional ^{123}I-IMP SPECT method for measuring CVR, which required arterial sampling and 2 days to perform, our split-dose ^{123}I-IMP SPECT method can be completed in ≈1 hour. During the short interval between the baseline and ACZ challenge tests, the physiological parameters (blood pressure, arterial pH, and $Paco_2$) should be stable, allowing the absolute CVR values to be calculated without arterial blood sampling for quantitative measurement of CBF.

In contrast to Powers'[23] theory, a negative correlation was observed between split-dose ^{123}I-IMP SPECT–measured CVR values and the OEF, suggesting that the OEF may be elevated even at the stage when the CVR response to ACZ is maintained. Several factors may contribute to this correlation between CVR and OEF. First, the OEF may begin to increase before the arteries reach maximal dilatation by autoregulation. This is supported by Derdeyn et al,[24] who observed patients with an increased OEF but without an increased CBV. Second, the vascular systems that dilate after a decrease in cerebral perfusion pressure or in response to an ACZ

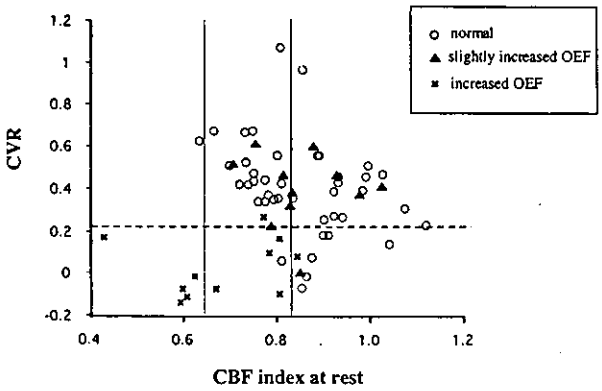

Figure 5. Detection of stage 2 cerebral hemodynamic failure by semiquantitative SPECT analysis on the affected side (group A). The lesions were classified into 3 groups according to their OEF values determined by PET, and each value was plotted on the basis of the CBF index at rest and CVR measured in the SPECT study. Neither the CBF index nor CVR alone was effective in detecting lesions with an elevated OEF. However, when a CVR cutoff value of 0.23 (mean−2 SD; broken line) and a CBF index cutoff value of 0.83 (normal value; thick line) were combined, a sensitivity of 82% (9 of 11), specificity of 96% (51 of 53), and a positive predictive value of 82% (9 of 11) were obtained.

challenge may be different.[17] Third, the ischemic brain tissue within the ROI may be heterogeneous, creating the possibility that regions of stage 1 and 2 hemodynamic failure may be mixed within the same ROI.

On the basis of the correlation between the split-dose ^{123}I-IMP SPECT–measured CVR values and the PET-measured OEF values, we attempted to clarify whether the CVR value alone could predict the existence of misery perfusion. Although the CVR cutoff value showed a high sensitivity (10 of 11, 91%) for the detection of misery perfusion (Figure 5), the positive predictive value was rather low (10 of 19, 53%). Because a significant correlation between CVR and CBF was not found in the PET study (Figure 3), we used the ^{123}I-IMP SPECT–measured CBF index represented as a cerebrum-to-cerebellum ratio to improve the positive predictive value of CVR for detecting misery perfusion. The SPECT-measured CBF index and the PET-measured CBF values were significantly correlated ($n=108$, $r=0.380$, $P<0.001$; data not presented). As expected from the results of Figure 3, the CBF indexes in ROIs below the CVR cutoff value (0.23) varied considerably (from 0.43 to 1.11). However, a combined CVR cutoff value (0.23) and a CBF index cutoff value of 0.83 produced a high sensitivity (9 of 11, 82%), specificity (51 of 53, 96%), and positive predictive value (9 of 11, 82%) for the detection of misery perfusion with an increased OEF (OEF >53.3%), as shown in Figure 5. We determined an abnormal CVR and CBF index with a 95% confidence limit from control subjects in the present study on the basis of the previous studies[3,10,20]; however, the pathophysiological relevance of a CVR and CBF index that is 2 SD from the mean is not necessarily clear and should be clarified in future studies. Five patients with bilateral carotid occlusive diseases were included in this study (the Table), but none of these patients exhibited an elevated OEF on their PET images. However, the combination of the CVR and CBF index (Figure 5) could potentially be applied for the detection of misery perfusion in both unilateral and bilateral carotid occlusive diseases.

In conclusion, split-dose ^{123}I-IMP SPECT can be potentially useful as a cost-effective, noninvasive tool to detect patients with misery perfusion. The combination of the CVR and CBF index can be a reliable index for accurately detecting the existence of increased OEF in both unilateral and bilateral carotid occlusive diseases.

Acknowledgments

We would like to thank the staff of the Department of Nuclear Medicine and the cyclotron staff of Osaka University Medical School Hospital for their technical support in performing the studies.

References

1. Yonas H, Smith HA, Durham SR, Pentheny SL, Johnson DW. Increased stroke risk predicted by compromised cerebral blood flow reactivity. *J Neurosurg.* 1993;79:483–489.
2. Grubb RL Jr, Derdeyn CP, Fritsch SM, Carpenter DA, Yundt KD, Videen TO, Spitznagel EL, Powers WJ. Importance of hemodynamic factors in the prognosis of symptomatic carotid occlusion. *JAMA.* 1998;280:1055–1060.
3. Yamauchi H, Fukuyama H, Nagahama Y, Nabatame H, Ueno M, Nishizawa S, Konishi J, Shio H. Significance of increased oxygen extraction fraction in five-year prognosis of major cerebral arterial occlusive diseases. *J Nucl Med.* 1999;40:1992–1998.
4. Powers WJ, Press GA, Grubb RL Jr, Gado M, Raichle ME. The effect of hemodynamically significant carotid artery disease on the hemodynamic status of the cerebral circulation. *Ann Intern Med.* 1987;106:27–34.
5. Baron JC, Bousser MG, Rey A, Guillard A, Comar D, Castaigne P. Reversal of focal "misery-perfusion syndrome" by extra-intracranial arterial bypass in hemodynamic cerebral ischemia: a case study with ^{15}O positron emission tomography. *Stroke.* 1981;12:454–459.
6. Hashikawa K, Matsumoto M, Moriwaki H, Oku N, Okazaki Y, Uehara T, Handa N, Kusuoka H, Kamada T, Nishimura T. Split dose iodine-123-IMP SPECT: sequential quantitative regional cerebral blood flow change with pharmacological intervention. *J Nucl Med.* 1994;35:1226–1233.
7. Hashikawa K, Matsumoto M, Moriwaki H, Oku N, Seike Y, Sakaguchi M, Sugimoto K, Nishimura H, Fukuchi K, Watanabe Y, Uehara T, Hori M, Nishimura T. Non-invasive measurement of cerebral perfusion reserve, split dose I-123 IMP SPECT method: the validation with O-15 H2O PET method. *J Nucl Med.* 1997;38:279. Abstract.
8. Kanno I, Uemura K, Higano S, Murakami M, Iida H, Miura S, Shishido F, Inugami A, Sayama I. Oxygen extraction fraction at maximally vasodilated tissue in the ischemic brain estimated from the regional CO_2 responsiveness measured by positron emission tomography. *J Cereb Blood Flow Metab.* 1998;8:227–235.
9. Herold S, Brown MM, Frackowiak RS, Mansfield AO, Thomas DJ, Marshall J. Assessment of cerebral haemodynamic reserve: correlation between PET parameters and CO_2 reactivity measured by the intravenous 133 xenon injection technique. *J Neurol Neurosurg Psychiatry.* 1988;51:1045–1050.
10. Hirano T, Minematsu K, Hasegawa Y, Tanaka Y, Hayashida K, Yamaguchi T. Acetazolamide reactivity on ^{123}I-IMP single photon emission computed tomography in patients with major cerebral artery occlusive disease: correlation with positron emission tomography parameters. *J Cereb Blood Flow Metab.* 1994;14:763–770.
11. Nariai T, Suzuki R, Hirakawa K, Maehara T, Ishii K, Senda M. Vascular reserve in chronic cerebral ischemia measured by the acetazolamide challenge test: comparison with positron emission tomography. *AJNR Am J Neuroradiol.* 1995;16:563–570.
12. North America Symptomatic Carotid Endarterectomy Trial Steering Committee. North America Symptomatic Carotid Endarterectomy Trial: methods, patient characteristics and progress. *Stroke.* 1991;22:711–720.
13. Whisnant JP, Basford JR, Bernstein EF. Classification of cerebrovascular disease III. *Stroke.* 1990;21:637–676.
14. Hauge A, Nicolaysen G, Thoresen M. Acute effects of acetazolamide on cerebral blood flow in man. *Acta Physiol Scand.* 1983;117:233–239.

15. Sullivan HG, Allison JD, Kingsbury TB 4th, Goode JJ. Analysis of inhalation rCBF data. *Stroke*. 1987;18:495–502.
16. Kazumata K, Tanaka N, Ishikawa T, Kuroda S, Houkin K, Mitsumori K. Dissociation of vasoreactivity to acetazolamide and hypercapnia: comparative study in patients with chronic occlusive major cerebral artery disease. *Stroke*. 1996;27:2052–2058.
17. Inao S, Tadokoro M, Nishino M, Mizutani N, Terada K, Bundo M, Kuchiwaki H, Yoshida J. Neural activation of the brain with hemodynamic insufficiency. *J Cereb Blood Flow Metab*. 1998;18:960–967.
18. Okazawa H, Yamauchi H, Sugimoto K, Toyoda H, Kishibe Y, Takahashi M. Effects of acetazolamide on cerebral blood flow, blood volume, and oxygen metabolism: a positron emission tomography study with healthy volunteers. *J Cereb Blood Flow Metab*. 2001;21:1472–1479.
19. Hayashida K, Hirose Y, Tanaka Y. Stratification of severity by cerebral blood flow, oxygen metabolism and acetazolamide reactivity in patients with cerebrovascular disease. In: Ishii Y, ed. *Recent Advances in Biomedical Imaging*. Amsterdam, Netherlands: Elsevier; 1997:113–119.
20. Yamauchi H, Fukuyama H, Kimura J, Konishi J, Kameyama M. Hemodynamics in internal carotid artery occlusion examined by positron emission tomography. *Stroke*. 1990;21:1400–1406.
21. Moriwaki H, Matsumoto M, Hashikawa K, Oku N, Ishida M, Seike Y, Watanabe Y, Hougaku H, Handa N, Nishimura T. Hemodynamic aspect of cerebral watershed infarction: assessment of perfusion reserve using iodine-123-iodoamphetamine SPECT. *J Nucl Med*. 1997;38:1556–1562.
22. Moriwaki H, Matsumoto M, Hashikawa K, Oku N, Ishida M, Seike Y, Fukuchi K, Hori M, Nishimura T. Iodine-123-iomazenil and iodine-123-iodoamphetamine SPECT in major cerebral artery occlusive disease. *J Nucl Med*. 1998;39:1348–1353.
23. Powers WJ. Cerebral hemodynamics in ischemic cerebrovascular disease. *Ann Neurol*. 1991;29:231–240.
24. Derdeyn CP, Grubb RL Jr, Powers WJ. Cerebral hemodynamic impairment: methods of measurement and association with stroke risk. *Neurology*. 1999;53:251–259.

ELSEVIER

Ultrasound in Med. & Biol., Vol. 29, No. 3, pp. 367–371, 2003

0301-5629/03/$–see front matter

doi:10.1016/S0301-5629(02)00743-3

● *Original Contribution*

EQUIVALENCE OF PLAQUE SCORE AND INTIMA-MEDIA THICKNESS OF CAROTID ULTRASONOGRAPHY FOR PREDICTING SEVERE CORONARY ARTERY LESION

MANABU SAKAGUCHI,* KAZUO KITAGAWA,* YOJI NAGAI,* HIROSHI YAMAGAMI,* KIMITO KONDO,* KOHJI MATSUSHITA,* NAOHIKO OKU,* HIDETAKA HOUGAKU,* TOSHIHO OHTSUKI,* TOHRU MASUYAMA,* MASAYASU MATSUMOTO† and MASATSUGU HORI*

*Department of Internal Medicine and Therapeutics (A8), Osaka University Graduate School of Medicine, Suita, Japan; and †Department of Clinical Neuroscience and Therapeutics, Hiroshima Graduate School of Biomedical Sciences, Hiroshima, Japan

(*Received* 1 *July* 2002; *in final form* 11 *November* 2002)

Abstract—Carotid atherosclerosis appears to be predictive of myocardial infarction. Because several sonographical indices are available for carotid ultrasound (US), we compared "blindly" the potential utilities of those indices for predicting coronary lesions in 270 patients. Carotid atherosclerosis was evaluated by the following four indices: plaque score (PlaS), intima-media thickness (IMT) of common carotid artery (CCA-IMT), IMT of bulb to internal carotid artery (Bulb-ICA-IMT), and combined IMT measurement from all segments. The existence of coronary lesions was diagnosed by > 50% stenosis in diameter in coronary arteries. All indices were associated with coronary lesions independent of risk factors. By receiver-operating characteristic (ROC) curve analyses, ROC areas defined by Bulb-ICA-IMT (0.76 to 0.86), combined IMT (0.76 to 0.86) and PS (0.76 to 0.87) were greater than that defined by CCA-IMT (0.64 to 0.76). In conclusion, PlaS, Bulb-ICA-IMT and combined IMT are equally effective and could be better than CCA-IMT for predicting coronary lesions in a population with cardiovascular risk. (E-mail: kitagawa@medone.med.osaka-u.ac.jp) © **2003 World Federation for Ultrasound in Medicine & Biology.**

Key Words: **Plaque score, Intima media thickness, Ultrasonography, Carotid atherosclerosis, Coronary artery lesion.**

INTRODUCTION

Carotid atherosclerosis as assessed by ultrasound (US) is often used as a surrogate for systemic atherosclerosis. Most epidemiologic and clinical studies are based on measurement of the intima-media thickness (IMT), a method first described by Pignoli et al. (1985). Previous cross-sectional studies have shown associations between IMT and the prevalence of cardiovascular disease (O'Leary et al. 1992; Burke et al. 1995; Allan et al. 1997). Recently, prospective studies showed that an increased IMT was associated with an increased risk of myocardial infarction and stroke (Salonen and Salonen 1991; Chambless et al. 1997; Bots et al. 1997; O'Leary et al. 1999).

Although IMT has been widely used as an index of carotid atherosclerosis, measurements of IMT varied considerably. Combined IMT measurements of common carotid artery (CCA), carotid bulb (Bulb) and internal carotid artery (ICA) have been used in the Cardiovascular Health Study (CHS) (O'Leary et al. 1991, 1999), Atherosclerosis Risk in Communities (ARIC) Study (Burke et al. 1995; Chambless et al. 1997), and the Asymptomatic Carotid Artery Plaque Study (Riley et al. 1992). In contrast, measurements of CCA-IMT have also been used in the Rotterdam Study (Bots et al. 1997), the Étude du Profil Génétique de l' Infarctus Cérébral (GÉNIC) Study (Touboul et al. 2000) and by several other investigators (Salonen and Salonen 1991; Nagai et al. 1998; Simons et al. 1999). Because it has been suggested that IMT of up to 1.0 mm may, in part, reflect an adaptive response to changes in tensile and shear stress (Bots et al.

Address correspondence to: Kazuo Kitagawa, M.D., Division of Stroke Research, Department of Internal Medicine and Therapeutics (A8), Osaka University Graduate School of Medicine, 2-2 Yamadaoka, Suita, Osaka 565-0871 Japan. E-mail: kitagawa@medone.med.osaka-u.ac.jp

1997), several investigators and study groups have used a plaque-scoring system (Crouse et al. 1986), where only atheromatous plaques were included and diffuse thickening of IMT of less than 1.0 mm was ignored. We also developed plaque score (PlaS) (Handa et al. 1990) and showed that PlaS categorization was useful for predicting future ischemic stroke events (Handa et al. 1995). There have only been a few studies comparing the strength of several indices of carotid atherosclerosis for the prediction of cardiovascular events. O'Leary et al. (1999) showed that combination of the CCA and ICA IMT was more strongly associated with the prevalence of cardiovascular disease, with traditional risk factors and with new cardiovascular events, than either variable used alone. However, it is unclear whether or not a plaque-scoring system such as PlaS is as good a predictor of the prevalence of cardiovascular disease and future cardiovascular events as several measurements of IMT.

We, therefore, measured several indices of carotid atherosclerosis and angiographic severity of coronary artery disease in 270 consecutive patients to compare the potential utilities of PlaS and several IMT measurements for predicting coronary lesions in a population with higher cardiovascular risk.

PATIENTS AND METHODS

Subjects

We studied 270 patients, 40 years old or older, who had consecutively undergone elective coronary angiography at our institute. Subjects were excluded when they had histories of carotid surgery or Takayasu's arteritis. Coronary angiography was performed for the evaluation of ischemic heart disease in 177 (65.6%), valvular heart disease in 61 (22.6%), cardiomyopathy in 8 (3.0%), congenital heart disease in 14 (5.2%) and others in 10 patients (3.7%). Informed consent was obtained from all the patients, and the institutional ethics committee approved the study. The investigation conforms to the principles outlined in the Declaration of Helsinki.

Before cardiac catheterization, the patients were asked to assess symptoms, risk factor profile, and current medical therapy.

For definition of risk factors, hypercholesterolemia was defined as total serum cholesterol $\geq$ 5.7 mmol/L or current use of lipid-lowering agents. Hypertension was defined as systolic blood pressure $\geq$ 140 mmHg and/or diastolic blood pressure $\geq$ 90 mmHg or current use of antihypertensive medication. Diabetes mellitus was defined as fasting plasma glucose $\geq$ 7.0 mmol/L, glycosylated hemoglobin (HbA1c) $\geq$ 5.8% or current use of hypoglycemic agents. Smoking status was categorically defined on the basis of self-reports, with a smoker defined by current or past smoking $\geq$ 10 cigarettes per day for $>$ 1 year.

Evaluation of vascular status

To evaluate the carotid atherosclerosis, high-resolution B-mode ultrasonography was performed with a 7.5-MHz linear-type probe (Toshiba SSA-260A CE, Tokyo, Japan). Three different longitudinal views (anterior oblique, lateral, and posterior oblique) and transverse views of both carotid systems were obtained. The IMT was evaluated as the distance between the luminal-intimal interface and the medial-adventitial interface, and it was measured with the use of an electronic caliper on the frozen frame of a suitable longitudinal image. The severity of carotid atherosclerosis was evaluated based on the following four indices: plaque score (PlaS), CCA-IMT, Bulb-ICA-IMT and combined IMT. These indicies of IMT are similar to those reported in the CHS (O'Leary et al. 1991; O'Leary et al. 1999), ARIC study (Burke et al. 1995; Chambless et al. 1997) and Rotterdam study (Bots et al. 1997). To obtain each index, the extracranial carotid artery was divided into four segments of 15 mm each with a flow divider and termed ICA (S1), carotid bulb (S2), beginning at the tip of the flow divider and extending 15 mm proximal, distal CCA (S3) and proximal CCA (S4), extending 15 to 30 mm and 30 to 45 mm proximal to the tip of the flow divider into the CCA (Fig. 1). To obtain the plaque score (PlaS), protruding lesions with an IMT $\geq$ 1.1 mm were defined as atheromatous plaque. PlaS was calculated by summing all the plaque thickness measurements in both carotid arteries (S1 to S4) (Handa et al. 1990; Nagai et al. 2001; Hashimoto et al. 2001). The IMT at each segment, except for the proximal CCA, was defined as the mean of the maximal wall thickness of the near and far wall on both the left and right sides. CCA-IMT was defined as the mean of the maximal wall thickness at the distal CCA (S3). Bulb-ICA-IMT was defined as the mean of the maximal wall thickness at eight points in the carotid bulb and ICA (S1 and S2). Combined IMT was defined as mean of the maximal wall thickness at 12 points in the distal CCA, carotid bulb, and ICA (S1, S2 and S3). All measurements (PlaS, CCA-IMT, Bulb-ICA-IMT, combined IMT) were performed by M. Sakaguchi. When intraobserver reproducibility was assessed for 30 patients, the interrater correlation of PlaS was 0.89, and 0.93 for CCA-IMT, 0.87 for Bulb-ICA-IMT, and 0.88 for combined IMT.

Coronary angiography was performed by the percutaneous technique using either the Judkins or multipurpose catheters. The patients were divided into those with coronary lesions when they showed $>$ 50% stenosis in diameter or occlusion in either of the coronary arteries (Scanlon and Faxon 1999). The patients with histories of coronary angioplasty or coronary artery bypass surgery

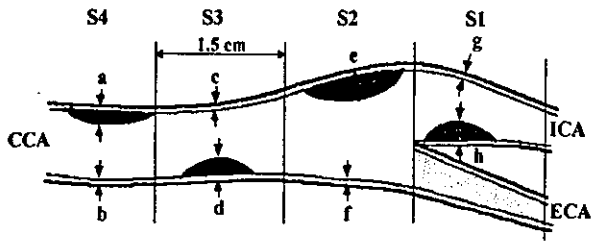

Fig. 1. Diagrams of carotid bifurcation and measurements obtained from B-mode ultrasonography. S1 = proximal internal carotid artery (ICA); S2 = carotid bulb; S3 = distal common carotid artery (CCA); S4 = proximal CCA. Shadowing is added within the vascular wall of external carotid artery (ECA). All measurements of plaque score and IMT were performed in the CCA, carotid bulb and ICA. Arrows outside the vascular wall indicate the measuring sites of either side for averaging IMT. The plaque score was calculated by summing all the plaque thickness measurements in both carotid arteries of S1, S2, S3 and S4 (a+d+e+h+ contralateral plaque). CCA-IMT was defined as the mean of the maximal wall thickness of the near and far wall on both the left and right sides at distal CCA of S3(*i.e.*, c+d+ contralateral sides/4). Bulb-ICA-IMT was defined as the mean of the maximal wall thickness at eight points in the carotid bulb and ICA (near and far walls on both sides of S1 and S2), (*i.e.*, e+f+g+h+ contralateral sides/8). Combined IMT was defined as the mean of the maximal wall thickness at 12 points (near and far walls on both sides of S1, S2 and S3), (*i.e.*, c+d+e+f+g+h+ contralateral sides/12).

were classified into those with coronary lesions. Angiographic findings were recorded by observers (T. Ohtsuki and T. Masuyama) who were "blinded" to the carotid PlaS and IMT values and whose only involvement in the study was recording the angiograms.

Statistical analysis

All statistical analyses were performed with SPSS/Windows System, version 9.0J (SPSS Japan Inc, Tokyo, Japan). All descriptive data are expressed as mean ± SD. Values of age, PlaS and IMT indices were compared with the unpaired *t*-test and the percentage of males, hypertension, hypercholesterolemia, diabetes mellitus and smokers was compared with the χ^2 test between the patients with and without coronary lesions. The ability of PlaS and each IMT index to predict coronary atherosclerosis was examined by logistic regression analysis after adjustment for cardiovascular risk factors, followed by ROC curve analyses.

RESULTS

The baseline characteristics of patients are shown in Table 1. Cardiovascular risk factors were more prevalent and all indices of carotid atherosclerosis were higher in the patients with coronary lesions than in those without (Table 1). Additionally, the prevalence of coronary lesions was examined by quartile of PlaS and each IMT index (Fig. 2). The prevalence increased with increasing quartiles for each index.

To examine the contribution of PlaS and each IMT index to predict coronary lesions, we performed logistic regression analyses and computed the odds ratios associated with 1 SD difference in PlaS and each IMT. In univariate analyses, each 1 SD greater than PlaS, CCA-IMT, Bulb-ICA-IMT and combined IMT was associated with a 5.4-fold, 2.7-fold, 5.2-fold and 5.3-fold higher risk of coronary lesions, respectively (Table 2). After adjustments for cardiovascular risk factors, all indices remained independently associated with coronary lesions.

Given these results, the ability of PlaS and each IMT index to predict coronary lesions was further examined by ROC curve analyses (Fig. 3). The ROC areas for PlaS (0.82; 95%CI, 0.76 to 0.87), Bulb-ICA-IMT (0.81; 95%CI, 0.76 to 0.86) and combined IMT (0.81; 95%CI,

Table 1. Baseline characteristics of subjects

Subjects	Total	Coronary lesions (+)	Coronary lesions (−)	*p* value
Number	270	186	84	–
Age (years mean ± SD)	63.4 ± 9.4	64.2 ± 9.5	61.6 ± 8.9	0.03
Male (%)	70	77	52	<0.0001
Hypertension (%)	58	67	39	<0.0001
Diabetes mellitus (%)	30	39	10	<0.0001
Hypercholesterolemia (%)	51	59	36	0.0003
Smoking (%)	60	70	38	<0.0001
Plaque score (mean ± SD)	11.2 ± 9.6	14.1 ± 9.5	4.6 ± 5.9	<0.0001
CCA-IMT (mm) (mean ± SD)	1.01 ± 0.40	1.08 ± 0.44	0.84 ± 0.25	<0.0001
Bulb-ICA-IMT (mm) (mean ± SD)	1.30 ± 0.51	1.46 ± 0.51	0.95 ± 0.30	<0.0001
Combined IMT (mm) (mean ± SD)	1.20 ± 0.42	1.33 ± 0.42	0.92 ± 0.25	<0.0001

Age, plaque score and respective indices of IMT are compared with the unpaired *t*-test and percentage of males, hypertension, hypercholesterolemia, diabetes mellitus and smoking is compared with the χ^2 test between the subjects with and without coronary lesions (> 50% stenosis in diameter or occlusion in either of coronary arteries). CCA = common carotid artery; ICA = internal carotid artery; IMT = intima-media thickness.

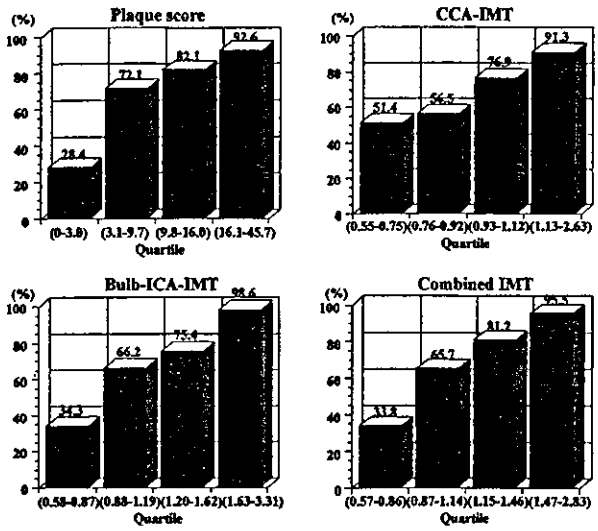

Fig. 2. Increasing frequency of coronary artery lesions according to quartile of plaque score and each IMT index.

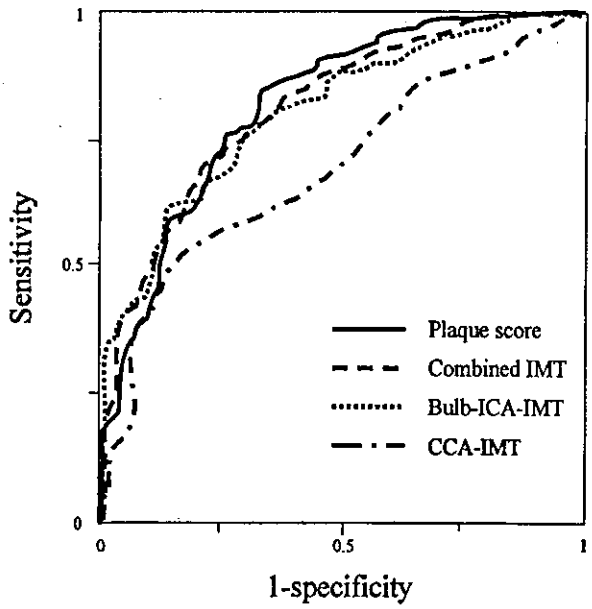

Fig. 3. ROC plots for use of plaque score and each IMT to predict the presence of coronary artery lesions. The areas under ROC curves for plaque score, Bulb-ICA-IMT and combined IMT were greater than those for CCA-IMT.

0.76 to 0.86) were greater than those for CCA-IMT (0.70; 95%CI 0.64 to 0.76).

DISCUSSION

Although we were aware that all indices of carotid atherosclerosis, PlaS and IMT indices, are associated with cardiovascular risk factors, we have shown that every index is a predictor of coronary lesions even after statistical adjustment for other risk factors. Previous studies examined the relation between B-mode US measurements of carotid atherosclerosis and coronary lesions. Craven et al. (1990) used the B-mode score, the sum of measurements of the maximum near and far wall thickness in the low common, high common, and low ICA on the left and right sides, and compared it between coronary patients and those who were not. They found the B-mode score to be strongly and independently associated with coronary artery disease in patients older than 50 years. Kallikazaros et al. (1999) also showed that carotid disease (lumen diameter stenosis of > 50%) was significantly correlated with severe coronary artery disease in patients with chest pain. In contrast, Adams et al. (1995) showed that CCA-IMT was only weakly associated with the severity of coronary atherosclerosis. However, there are no published data to indicate which index of carotid atherosclerosis with the B-mode is the most sensitive or specific for predicting coronary atherosclerosis.

Table 2. Odds ratio for coronary lesions as a function of a 1-SD difference in one of the indices of carotid atherosclerosis

Variable	Relative Risk (95% CI) Unadjusted	Adjusted for age, gender and other risk factors*
Plaque score	5.42 (3.32–8.84)	4.54 (2.55–8.08)
CCA-IMT	2.71 (1.74–4.22)	2.03 (1.27–3.25)
Bulb-ICA-IMT	5.24 (3.27–8.38)	4.65 (2.63–8.23)
Combined IMT	5.25 (3.26–8.45)	4.94 (2.71–9.02)

*Other risk factors are hypertension, diabetes mellitus, hypercholesterolemia and smoking. CCA = common carotid artery; ICA = internal carotid artery; IMT = intima-media thickness; CI = confidence interval.

The present study suggested that both PlaS and IMT, indices including carotid bulb and ICA, are more strongly associated with coronary lesions than CCA-IMT. Furthermore, PlaS is at least as good a predictor of coronary atherosclerosis as carotid bulb to ICA IMT indices commonly used in large clinical trials such as CHS (O'Leary et al. 1991) and the ARIC study (Burke et al. 1995). Because focal plaques are more frequent in the carotid bulb and ICA, compared to CCA, it is likely that PlaS and carotid bulb to ICA IMT indices more directly reflect them than CCA-IMT.

The main limitation of this study was that the subjects were not population-based. It remains unclear whether or not PlaS is as good a predictor of coronary atherosclerosis in healthy individuals and in the patients without histories of cardiovascular events as IMT, which CHS and ARIC study groups used. Furthermore, it should be taken into account that more than 80% of patients in the present study showed atheromatous

plaques in the carotid arteries. PlaS may be an effective index to predict coronary lesions, especially in elderly patients with higher cardiovascular risk. However, in a healthy, middle-aged population, carotid atherosclerosis is generally minimal, but myocardial infarction could occur in those people. In that population, PlaS may have a low sensitivity and IMT measurement of diffuse intima-media thickening at CCA may be a better predictor of coronary lesions or events. Furthermore, CCA-IMT measurements are quicker, more accurate and more reproducible than PlaS and bulb-to-ICA IMT indices. It may be worthwhile to compare indices in terms of easiness to measure intra- and interobserver variabilities. It may be of interest, too, to investigate the possible superiority of indices extracted from 3-D scans. We should properly use the various indices of carotid atherosclerosis according to different groups of subjects.

SUMMARY

PlaS and mean value of maximal IMT in the CCA, carotid bulb and ICA are equally effective and could be better indices than CCA-IMT to predict coronary atherosclerosis. The plaque-scoring system such as PlaS may be one of the best indices to screen individuals with coronary atherosclerosis when patients with several risk factors are managed in the hospital.

Acknowledgements—This study was supported in part by Research Grants for Cardiovascular Diseases from the Ministry of Health, Labour and Welfare, and from the Smoking Research Foundation of Japan. We are grateful to Miss R. Morimoto and Miss S. Imoto for secretarial assistance.

REFERENCES

Adams MR, Nakagomi A, Keech A, et al. Carotid intima-media thickness is only weakly correlated with the extent and severity of coronary artery disease. Circulation 1995;92:2127–2134.

Allan PL, Mowbray PI, Lee AJ, Gerald F, Fowkes R. Relationship between carotid intima-media thickness and symptomatic and asymptomatic peripheral arterial disease: The Edinburgh Artery Study. Stroke 1997;28:348–353.

Bots ML, Hofman A, Grobbee DE. Increased common carotid intima-media thickness: Adaptive response or a reflection of atherosclerosis? Findings from the Rotterdam Study. Stroke 1997;28:2442–2447.

Bots ML, Hoes AW, Koudstaal PJ, Hofman A, Grobbee DE. Common carotid intima-media thickness and risk of stroke and myocardial infarction: The Rotterdam Study. Circulation 1997;96:1432–1437.

Burke GL, Evans GW, Riley WA, et al. Arterial wall thickness is associated with prevalent cardiovascular disease in middle-aged adults: The Atherosclerosis Risk in Communities (ARIC) study. Stroke 1995;26:386–391.

Chambless LE, Heiss G, Folsom AR, et al. Association of coronary heart disease incidence with carotid wall thickness and major risk factors: The Atherosclerosis Risk in Communities (ARIC) Study, 1987–1993. Am J Epidemiol 1997;146:483–494.

Craven TE, Ryu JE, Espeland MA, et al. Evaluation of the associations between carotid artery atherosclerosis and coronary artery stenosis. A Case-control study. Circulation 1990;82:1230–1242.

Crouse JR, Harpold GH, Kahl FR, Toole JF, McKinney WM. Evaluation of a scoring system for extracranial carotid atherosclerosis extent with B-mode ultrasound. Stroke 1986;17:270–275.

Handa N, Matsumoto M, Maeda H, et al. Ultrasonic evaluation of early carotid atherosclerosis. Stroke 1990;21:1567–1572.

Handa N, Matsumoto M, Maeda H, Hougaku H, Kamada T. Ischemic stroke events and carotid atherosclerosis. Stroke 1995;26:1781–1786.

Hashimoto H, Kitagawa K, Hougaku H, et al. C-reactive protein is an independent predictor of the rate of increase in early carotid atherosclerosis. Circulation 2001;104:63–67.

Kallikazaros I, Tsioufis C, Sideris S, Stefanadis C, Toutouzas P. Carotid artery disease as a marker for the presence of severe coronary artery disease in patients evaluated for chest pain. Stroke 1999;30:1002–1007.

Nagai Y, Kitagawa K, Sakaguchi M, et al. Significance of earlier carotid atherosclerosis for stroke subtypes. Stroke 2001;32:1780–1785.

Nagai Y, Metter J, Earley CJ, et al. Increased carotid artery intima-medial thickness in asymptomatic older subjects with exercise-induced myocardial ischemia. Circulation 1998;98:1504–1509.

O'Leary DH, Polak JF, Wolfson SK, et al. Use of sonography to evaluate carotid atherosclerosis in the elderly. The Cardiovascular Health Study. Stroke 1991;22:1155–1163.

O'Leary DH, Polak JF, Kronmal RA, et al., on behalf of the CHS Collaborative Research Group: Distribution and correlates of sonographically detected carotid artery disease in the cardiovascular health study. Stroke 1992;23:1752–1760.

O'Leary DH, Polak JF, Kronmal RA, for the Cardiovascular Health Study Collaborative Research Group. Carotid-artery intima and media thickness as a risk factor for myocardial infarction and stroke in older adults. N Engl J Med 1999;340:14–22.

Pignoli P, Tremoli E, Poli A, Oreste P, Paoletti R. Intimal plus medial thickness of the arterial wall: A direct measurement with ultrasound imaging. Circulation 1985;74:1399–1406.

Riley WA, Barnes RW, Applegate WB, et al. Reproducibility of noninvasive ultrasonic measurement of carotid atherosclerosis. The Asymptomatic Carotid Artery Plaque Study. Stroke 1992;23:1062–1068.

Salonen R, Salonen JT. Ultrasonographically assessed carotid morphology and the risk of coronary heart disease. Arterioscler Thromb 1991;11:1245–1249.

Scanlon PJ, Faxon DP. ACC/AHA guidelines for coronary angiography. A report of the American College of Cardiology/American Heart Association Task Force on Practice Guidelines (Committee on Coronary Angiography). J Am Coll Cardiol 1999;33:1756–1824.

Simons PC, Algra A, Bots ML, Grobbee DE, van der Graaf Y. Common carotid intima-media thickness and arterial stiffness: Indicators of cardiovascular risk in high-risk patients. The SMART Study (Second Manifestations of ARTerial disease). Circulation 1999;100:951–957.

Touboul PJ, Elbaz A, Koller C, et al., for the GÉNIC Investigators. Common carotid artery intima-media thickness and brain infarction. The Étude du Profil Génétique de l' Infarctus Cérébral (GÉNIC) Case-Control Study. Circulation 2000;102:313–318.

Circulating adhesion molecules are correlated with ultrasonic assessment of carotid plaques

Hiroyuki HASHIMOTO, Kazuo KITAGAWA, Keisuke KUWABARA, Hidetaka HOUGAKU, Toshiho OHTSUKI, Masayasu MATSUMOTO and Masatsugu HORI

Department of Internal Medicine and Therapeutics, Osaka University Graduate School of Medicine, 2-2 Yamadaoka, Suita, Osaka 565-0871, Japan

ABSTRACT

The relationship between levels of circulating intercellular cell-adhesion molecule-1 (cICAM-1) or P-selectin (cP-selectin) and the severity of carotid atherosclerosis was examined in 301 outpatients undergoing duplex ultrasonographic examination. Carotid plaque was defined as an intima-media thickness greater than 1.0 mm, and a plaque score (PS) was calculated from the plaque thickness in both carotid arteries. Multivariate analysis demonstrated significant positive associations between cICAM-1 and the number of plaques [$\beta = 0.11$; confidence interval (CI), 0.007–0.213], maximum intima-media thickness ($\beta = 0.11$; CI, 0.01–0.219), and PS ($\beta = 0.10$; CI, 0.001–0.205). In contrast, no significant association was found for cP-selectin. cP-selectin did not increase until atherosclerosis was advanced (PS > 10), showing a marked increase in patients with $\geqslant 50\%$ stenosis. The circulating levels of both proteins are related to real measurements of plaque formation in the carotid arteries independently of classical risk factors. Marked elevation of cP-selectin occurs in advanced carotid atherosclerosis after gradual elevation of cICAM-1.

INTRODUCTION

In vitro and animal experiments have demonstrated that adherence of circulating leucocytes to endothelial cells and subsequent transendothelial migration are critical steps in the early stages of atherosclerosis [1]. Recent clinical investigations have focused on the relationship between the levels of circulating leucocyte–endothelial adhesion molecules and cardiovascular disease (CVD). Among the various circulating adhesion molecules, circulating intercellular cell-adhesion molecule-1 (cICAM-1) has received the most attention, and two large-scale studies have demonstrated that an elevated cICAM-1 level is a predictor of future cardiovascular events [2,3]. With respect to other leucocyte–endothelial adhesion molecules, several experimental and histological studies have shown a close relationship between P-selectin and ICAM-1, and some studies have revealed that circulating P-selectin (cP-selectin) levels are higher in patients who suffer a subsequent cardiovascular event than in patients who do not [4–6]. Of the other circulating adhesion molecules, cP-selectin is the strongest predictor of the risk of cardiovascular events after cICAM-1 [7].

Detection of carotid atherosclerosis is useful because it is an indicator of generalized atherosclerosis [8–11] and a reliable predictor of future CVD [12–15]. However, studies investigating the relationship between circulating levels of the above adhesion molecules and carotid atherosclerosis had different population sizes and different indicators to estimate the severity of

Key words: adhesion molecule, atherosclerosis, carotid artery, circulating intercellular cell-adhesion molecule-1 (cICAM-1), circulating P-selectin (cP-selectin), inflammation, ultrasound.

Abbreviations: (c)ICAM-1, (circulating) intercellular cell-adhesion molecule-1; CI, confidence interval; cP-selectin, circulating P-selectin; HbA_{1c}, glycated haemoglobin; HDL, high-density lipoprotein; PS, plaque score; CVD, cardiovascular disease; IMT, intima-media thickness.

Correspondence: Dr Hiroyuki Hashimoto, Department of Internal Medicine, Osaka National Hospital 2-1-14, Hoenzaka, Chuoku, Osaka 540-0006, Japan (e-mail hashih@onh.go.jp).

carotid atherosclerosis, and therefore yielded inconsistent findings [2,16–21].

We have previously established the plaque score (PS) as an indicator of the severity of carotid atherosclerosis, and have investigated the relationships between this score and classical risk factors for CVD [22] and C-reactive protein [23], silent brain infarction [9], platelet accumulation in the carotid arteries [24] and future ischaemic cerebrovascular disease [14]. In the present study, we used the PS and several other indicators to estimate the severity of carotid atherosclerosis, and we investigated the relationship between cICAM-1 or cP-selectin levels and the severity of carotid atherosclerosis.

MATERIALS AND METHODS

Subjects

A total of 301 outpatients over 40 years old, who were being treated for classical risk factors and/or secondary prevention of CVD at the Department of Internal Medicine of Osaka University Hospital, were investigated for carotid atherosclerosis and provided blood samples. Patients were excluded from the study if they had experienced a clinical cardiovascular event in the previous year or if another disease that could increase the cICAM-1 or cP-selectin level was present, i.e. malignancy, collagen disease, chronic renal failure, infection or hepatic disease [25]. None of the subjects were receiving anti-oxidant vitamin supplements, oestrogen therapy or steroid therapy. Patients gave written informed consent to provide blood samples and participate in the study. The study was approved by the local ethics committees.

Risk factors for CVD

Hypertension was defined as a systolic blood pressure $\geqslant 140$ mmHg and/or a diastolic blood pressure $\geqslant 90$ mmHg, or the current use of antihypertensive medications. Hypercholesterolaemia was defined as total cholesterol level $\geqslant 220$ mg/dl or the current use of cholesterol-lowering agents. Diabetes mellitus was defined as a glycated haemoglobin (HbA_{1c}) level $\geqslant 5.8$ % or the current use of oral hypoglycaemic agents. Patients were considered to be smokers if they were current smokers or had stopped smoking less than 1 month before enrolment in the study. Cigarette pack-years were calculated for each patient as a measure of cumulative smoking exposure. Patients were considered to have CVD if they had a prior history of ischaemic heart disease, cerebrovascular disease, aortic aneurysm or peripheral vascular disease. Patients were defined as taking antiplatelet therapy if they were being treated with aspirin or ticlopidine.

Evaluation of carotid atherosclerosis and measurement of cICAM-1 and cP-selectin levels

High-resolution B-mode ultrasonography was performed with a 7.5-MHz duplex-type scanner (Hitachi EUB-450, 555) to evaluate carotid atherosclerosis. The upper limit of normal for the intima-media thickness (IMT) was defined as 1.0 mm [22], and lesions with an IMT $\geqslant 1.1$ mm were defined as atheromatous plaques. We used the following indicators to assess the severity of carotid atherosclerosis: (1) maximum IMT measured in mm at the thickest point (including plaque) of the near and far walls of both carotid arteries, (2) the number of plaques in both carotid arteries, (3) the PS (calculated by summing all plaque thicknesses measured in both carotid arteries, as shown in Figure 1) [22], and (4) the maximum stenosis (calculated by measuring the residual luminal diameter and the original diameter at the site of maximum stenosis and dividing the difference by the original diameter, with the result being reported as a percentage).

Blood samples were collected into tubes containing citric acid and EDTA, and were stored at −80 °C after centrifugation. The stored serum samples were assayed for cICAM-1, whereas the stored plasma samples were assayed for cP-selectin. Commercially available monoclonal antibody-based ELISA kits (R & D Systems, Minneapolis, MN, U.S.A.) were used for the determination of cICAM-1 and cP-selectin levels.

Statistical analysis

Data for the cICAM-1 and cP-selectin levels showed a normal distribution, whereas the maximum IMT, the number of plaques and the PS showed a skewed distribution. For univariate analysis, Spearman's rank-order correlation coefficients were determined to assess the association between cICAM-1 or cP-selectin level and the parameters of carotid atherosclerosis, i.e. maximum IMT, number of plaques and PS. The associations between

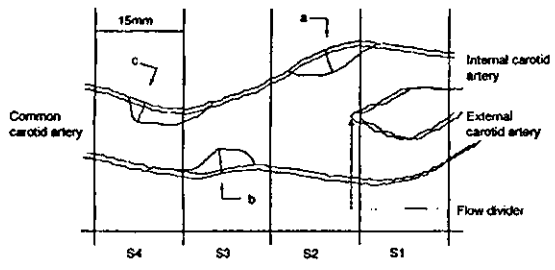

Figure 1 Diagram of carotid bifurcation and PS measurement obtained from B-mode ultrasonography

PS was calculated by summing all plaque thicknesses in mm in each segment on both sides (a + b + c + contralateral plaques). The carotid artery was divided into four parts, each 15 mm in length, from the flow divider (S1 to S4).

measured risk factors and PS were evaluated similarly. Differences of PS and the levels of circulating adhesion molecules in relation to categorical risk factors were evaluated by the Mann-Whitney U test and the unpaired t test respectively. Pearson's test was used to evaluate the relationship between cICAM-1 and cP-selectin levels, as well as those between the levels of these molecules and age. Patients were classified into four groups on the basis of the severity of carotid atherosclerosis: no disease (PS = 0), mild disease (PS = 1.1–5.0), moderate disease (PS = 5.1–10) and severe disease (PS > 10) [9,14,24]. One-way ANOVA was performed with Scheffé's multiple comparison test to assess differences in cICAM- and cP-selectin levels between these four groups. Patients were also classified into three groups on the basis of their maximum stenosis, i.e. no carotid atherosclerosis, less than 50% stenosis and 50% or more stenosis, after which the differences in cICAM-1 and cP-selectin levels between these three groups were similarly evaluated. To evaluate the differences, cICAM-1 and cP-selectin levels were adjusted for classical risk factors, statin use and a history of CVD. For multivariate analysis, multiple linear regression analysis was performed using each carotid atherosclerosis parameter as a dependent variable, while the age, sex, cigarette pack-years, presence/absence of hypertension, diabetes, hypercholesterolaemia, statin use, a history of CVD and the levels of circulating adhesion molecules were used as the predictive variables. The values of the maximum IMT, number of plaques and PS were log-transformed to normalize their distribution. 0.1 was assigned when number of plaques was 0, and 1.0 was assigned when PS was 0. All P values calculated were two-tailed and $P < 0.05$ was considered significant. All statistical analyses were conducted using SPSS/Windows software, version 9.0J (SPSS Japan Inc., Tokyo, Japan).

RESULTS

The clinical characteristics of the subjects are shown in Table 1. Of the 301 patients, 227 (75%) had carotid atherosclerosis, and 105 (35%) had a history of CVD and most of them were on antiplatelet therapy. In outpatients who were treated for hypertension, hypercholesterolaemia and diabetes mellitus, there were no significant differences in cICAM-1 and cP-selectin levels between the patients with or without these classical risk factors. As expected, the cICAM-1 level of current smokers was higher than that of non-current smokers (244.0 ± 86.1 ng/ml versus 189.0 ± 71.5 ng/ml, $P = 0.007$). The difference for cP-selectin was also significant (46.7 ± 26.5 ng/ml versus 38.5 ± 21.4 ng/ml, $P = 0.03$). The cICAM-1 level was higher in men than in women (212.8 ± 83.0 ng/ml versus 182.6 ± 66.3 ng/ml, $P = 0.008$), but no sex difference was found for cP-selectin. There were no statistical associations between the levels of the circulating adhesion molecules and age, nor were there any significant differences in cICAM-1 and cP-selectin levels between subjects with or without statin use, antiplatelet therapy or a history of CVD. The associations between the levels of cICAM-1 or cP-selectin and age were not significant when they were adjusted for gender. There was a significant correlation between cICAM-1 and cP-selectin levels ($r = 0.292$, $P < 0.001$).

Table 1 Clinical characteristics of the patients ($n = 301$)

Age, blood pressure, cholesterol, fasting blood glucose, HbA_{1c}, cigarette pack-years, plaque number, PS and circulating levels of adhesion molecules are expressed as the means ± S.D. Values shown in square brackets and parentheses are median values and number of patients respectively.

Characteristic	Value
Classical risk factors for CVD	
Age (years) (range)	64.0 ± 9.1 (40–88)
Male	53%
Hypertension	68%
Systolic/diastolic blood pressure (mmHg)	136 ± 17/80 ± 11
Hypercholesterolaemia	48%
Total cholesterol/HDL cholesterol (mg/dl)	207 ± 32/55 ± 17
Statin use	26%
Diabetes mellitus	18%
Fasting blood glucose (mg/dl)	104 ± 26
HbA_{1c} (%)	5.3 ± 0.9
Current smoker	17%
Cigarette pack-years	11.1 ± 22.2
History of CVD	35%
Antiplatelet medication	33%
Severity of carotid atherosclerosis	
Maximum IMT (mm)	1.9 ± 1.2 [1.5]
Number of plaques	2.7 ± 2.8 [2.0]
PS	4.8 ± 5.4 [2.9]
Maximum stenosis (0%, < 50%, ⩾ 50%)	(74, 200, 27)
cICAM-1 (ng/ml)	198.3 ± 76.8
cP-selectin (ng/ml)	39.9 ± 22.5

cICAM-1 and cP-selectin levels are shown in relation to the PS and maximum stenosis in Tables 2 and 3 respectively. Because the PS involves the factors of the number of plaques and maximum IMT, we showed Table 2 as a representative of the indicators. Unlike cICAM-1, cP-selectin did not increase until carotid atherosclerosis was severe (PS > 10). The cICAM-1 level of the severe group (PS > 10) was significantly higher than those of the group without atherosclerosis (PS = 0) and the group with mild atherosclerosis (PS = 1.1–5.0), whereas the cP-selectin level of the severe group was significantly higher than in all of the other three groups. The differences remained significant after adjustment for

Table 2 cICAM-1 and cP-selectin levels with respect to atherosclerosis categories

Values (except adjusted ones) are expressed as the means ± S.D. The adjusted values are expressed as the means ± S.E.M. *Adjusted for age, sex, smoking, hypertension, hypercholesterolaemia, statin use, diabetes mellitus and antiplatelet medication. †cICAM-1 levels in the severe disease group were significantly higher than levels in the none and mild disease groups ($P < 0.05$), but a significant difference was not found for the moderate disease group. ‡The differences remained significant after adjustment for classical risk factors, statin use and antiplatelet medication ($P < 0.05$). §cP-selectin levels in the severe disease group were higher than levels in the none, mild and moderate disease groups ($P < 0.05$).

Disease category	cICAM-1 (ng/ml)	Adjusted cICAM-1 (ng/ml)*	cP-selectin (ng/ml)	Adjusted cP-selectin (ng/ml)*
None ($n = 74$)	186.3 ± 80.7	188.2 ± 9.3	38.0 ± 24.5	38.0 ± 2.8
Mild ($n = 127$)	187.2 ± 75.1	188.1 ± 6.6	39.1 ± 19.7	39.2 ± 2.0
Moderate ($n = 49$)	218.3 ± 74.4	212.1 ± 11.0	35.9 ± 22.8	34.8 ± 3.3
Severe ($n = 51$)	224.2 ± 69.0†	227.8 ± 11.2‡	48.5 ± 24.5§	49.4 ± 3.4‡

Table 3 cICAM-1 and cP-selectin levels with respect to maximum stenosis

Values (except adjusted ones) are expressed as the means ± S.D. Adjusted values are expressed as the means ± S.E.M. *Adjusted for age, sex, smoking, hypertension, hypercholesterolaemia, statin use, diabetes mellitus and antiplatelet medication. cICAM-1 levels had a tendency to increase in parallel ($P = 0.067$), but the difference in the levels showed no statistical significance. †cP-selectin levels were higher in patients with 50% or more stenosis than in patients without carotid atherosclerosis and in patients with less than 50% stenosis ($P < 0.05$). ‡The difference remained significant after adjustment for classical risk factors, statin use and antiplatelet medication ($P < 0.05$).

Stenosis	cICAM-1 (ng/ml)	Adjusted cICAM-1 (ng/ml)*	cP-selectin (ng/ml)	Adjusted cP-selectin (ng/ml)*
0% ($n = 74$)	186.1 ± 80.2	190.3 ± 9.3	37.9 ± 24.3	38.1 ± 2.8
< 50% ($n = 200$)	199.2 ± 72.9	198.7 ± 5.4	38.9 ± 20.5	38.9 ± 1.6
⩾ 50% ($n = 27$)	225.9 ± 89.9	221.3 ± 14.8	53.2 ± 27.5†	52.2 ± 4.4‡

classical risk factors, statin use and antiplatelet medication (Table 2). When the number of plaques or maximum IMT was used as an indicator of carotid atherosclerosis, the results (not shown) were similar to those in Table 2. When maximum stenosis was used as an indicator of carotid atherosclerosis, cP-selectin levels were higher in patients with 50% or more stenosis than in patients without carotid atherosclerosis or patients with less than 50% stenosis. The difference remained significant after adjustment for classical risk factors, statin use and antiplatelet medication. cICAM-1 levels tended to increase in parallel with stenosis, although the trend was not statistically significant (Table 3).

Relationships between risk factors (including cICAM-1 and cP-selectin) and the PS are shown in Table 4. As expected, the PS of patients with classical risk factors and a history of CVD was higher than that in patients without these factors. The influence of cICAM-1 on the PS was similar to the influence of systolic blood pressure, high-density lipoprotein (HDL) cholesterol, fasting blood glucose, HbA_{1c} or cigarette pack-years. The influence of cP-selectin was weaker than that of the above risk factors, but it was still statistically significant. Diastolic blood pressure and total cholesterol were not significantly related to PS. When the predictive value of cICAM-1 or cP-selectin levels for the PS was compared with that of classical risk factors using multivariate regression analysis, the relationship between the cICAM-1 level and PS remained significant even after accounting for

Table 4 Relationships between PS and risk factors, including cICAM-1 and cP-selectin levels

The values shown are correlation coefficients between measured risk factors and PS, and mean ± S.D. for PS according to the presence or absence of categorical risk factors. n.s., not significant.

Risk factor for atherosclerosis	PS	P value
Age (years)	$r = 0.381$	< 0.001
Men/women	5.8 ± 6.0/3.6 ± 4.4	0.001
Hypertension (yes/no)	5.4 ± 3.8/3.2 ± 3.8	0.002
Systolic blood pressure	$r = 0.196$	0.001
Diastolic blood pressure	$r = -0.019$	n.s.
Hypercholesterolaemia (yes/no)	5.3 ± 5.5/4.3 ± 5.3	0.011
Total cholesterol	$r = 0.055$	n.s.
HDL cholesterol	$r = -0.167$	0.004
Statin use (yes/no)	5.6 ± 5.2/4.4 ± 5.4	0.01
Diabetes mellitus (yes/no)	7.1 ± 5.4/4.3 ± 5.3	< 0.001
Fasting blood glucose	$r = 0.197$	0.001
HbA_{1c}	$r = 0.239$	< 0.001
Current smoking (yes/no)	6.2 ± 6.0/4.5 ± 5.2	0.022
Cigarette pack-years	$r = 0.199$	0.001
History of CVD (yes/no)	6.1 ± 5.6/4.1 ± 5.2	0.001
cICAM-1	$r = 0.208$	< 0.001
cP-selectin	$r = 0.126$	0.03